# Single photon at a configurable quantum-memory-based beam splitter

Xianxin Guo, Yefeng Mei, and Shengwang Du*

*Department of Physics, The Hong Kong University of Science and Technology, Clear Water Bay, Kowloon, Hong Kong, China*

(Received 31 January 2018; published 5 June 2018)

We report the demonstration of a configurable coherent quantum-memory-based beam splitter (BS) for a single-photon wave packet making use of laser-cooled $^{85}$Rb atoms and electromagnetically induced transparency. The single-photon wave packet is converted (stored) into a collective atomic spin state and later retrieved (split) into two nearly opposing directions. The storage time, beam-splitting ratio, and relative phase are configurable and can be dynamically controlled. We experimentally confirm that such a BS preserves the quantum particle nature of the single photon and the coherence between the two split wave packets of the single photon.

DOI: 10.1103/PhysRevA.97.063805

## I. INTRODUCTION

Beam splitters (BSs), as one type of the most common and essential linear-optical components, have been widely used and thoroughly investigated in both fundamental research and engineering applications. They are particularly important elements for building amplitude-splitting interferometers [1–4], such as Mach-Zehnder (MZ) interferometer, Michelson interferometer, Sagnac ring interferometer, etc. In quantum optics, BSs act as keys for revealing nonclassical photon correlations and intriguing quantum nature of single photons, with typical examples of the Hanbury Brown–Twiss experiment [5] and the Hong-Ou-Mandel interference [6]. BSs are also important ingredients in photonic entanglement generation, distribution, and analysis [7], thus interconnecting different quantum nodes to form the backbone of a quantum computer [8] or a quantum network [9]. On the other hand, quantum memory, which allows on-demand interconversion between flying and stationary qubits, is another necessity in building up a practical quantum network [10]. Therefore, integration of the BS with quantum memory marks an important step toward scalable quantum networks. Recently, dynamical temporal BSs have been demonstrated based on Raman memory [11] and electromagnetically induced transparency (EIT) [12]. Xiao *et al.* demonstrated a BS using EIT coherence with flying atoms in a hot vapor cell [13]. These experiments all work with coherent classical pulses, so whether the quantum properties of single photons is preserved or modified in such active systems remains a question. One of the challenges to address this is to obtain narrow-band single photons matching the atomic transitions, because the efficient atom-photon interaction in those memory-based BS requires sufficiently narrower bandwidth of single photons as compared to a conventional passive BS.

In this paper, we produce narrow-band heralded single photons from one cold atomic ensemble and demonstrate a dynamical BS for single-photon wave packet based on EIT quantum memory in a second cold atomic ensemble. The input photon state $|\Psi_{\text{in}}\rangle$ is first stored in the quantum memory and then read out as a superposition state of two different momentum modes ($\vec{k}_1$ and $\vec{k}_2$) with forward and backward simultaneous retrieval:

$$|\Psi_{\text{in}}\rangle \rightarrow |\Psi_{\text{out}}\rangle = A[\cos\theta|\vec{k}_1\rangle + e^{i\varphi}\sin\theta|\vec{k}_2\rangle], \qquad (1)$$

where $A$ represents the total transmission and $\varphi$ is the relative phase between the two modes. The splitting ratio and relative phase can be dynamically controlled. With narrow-band heralded single photons, we confirm the single-photon particle nature on the BS with the antibunching effect and verify the phase coherence in a MZ interferometer.

## II. EXPERIMENTAL SETUP

Our experimental setup and relevant $^{85}$Rb atomic energy level diagrams are illustrated in Fig. 1. Backward time-frequency entangled Stokes and anti-Stokes photon pairs are produced from spontaneous four-wave mixing with $^{85}$Rb atoms in a dark-line two-dimensional (2D) magneto-optical trap (MOT) in site A with counterpropagating pump and coupling laser beams [14,15]. The optical depth (OD) of the cold atoms at MOT A is 40 on the anti-Stokes transition $|1\rangle \rightarrow |3\rangle$.The pump and coupling laser beams, with the same beam diameter ($1/e^2$ intensity) of 1.5 mm, are aligned with 3° angle to the Stokes and anti-Stokes directions. The pump laser (780 nm, Rabi frequency $2\pi \times 3$ MHz)) is blue detuned by 60 MHz from the transition $|1\rangle \rightarrow |4\rangle$, and the coupling laser (795 nm, Rabi frequency $2\pi \times 14$ MHz) is on resonance to the transition $|2\rangle \rightarrow |3\rangle$. These generated narrrow-band photons have a bandwidth of 5 MHz. Upon detecting a Stokes photon at a single-photon-counting module ($\text{SPCM}_s$) with a time resolution of 4 ns, we project the anti-Stokes photon in a highly pure temporal quantum state [16,17]. The heralded anti-Stokes photon, with its central frequency on resonance to the transition $|1\rangle \rightarrow |3\rangle$, is then coupled into a 110-m single-mode fiber and sent into a second $^{85}$Rb MOT at site B (MOT B) along the longitudinal $z$ axis. The OD of MOT B is 70 at the anti-Stokes transition $|1\rangle \rightarrow |3\rangle$. In site B, a control laser beam with a beam diameter of 1.5 mm, which is on resonance to the transition $|2\rangle \rightarrow |3\rangle$, passes through an electro-optic amplitude modulator (EOAM) and is split after a 50:50 BS into

*Corresponding author: dusw@ust.hk

 

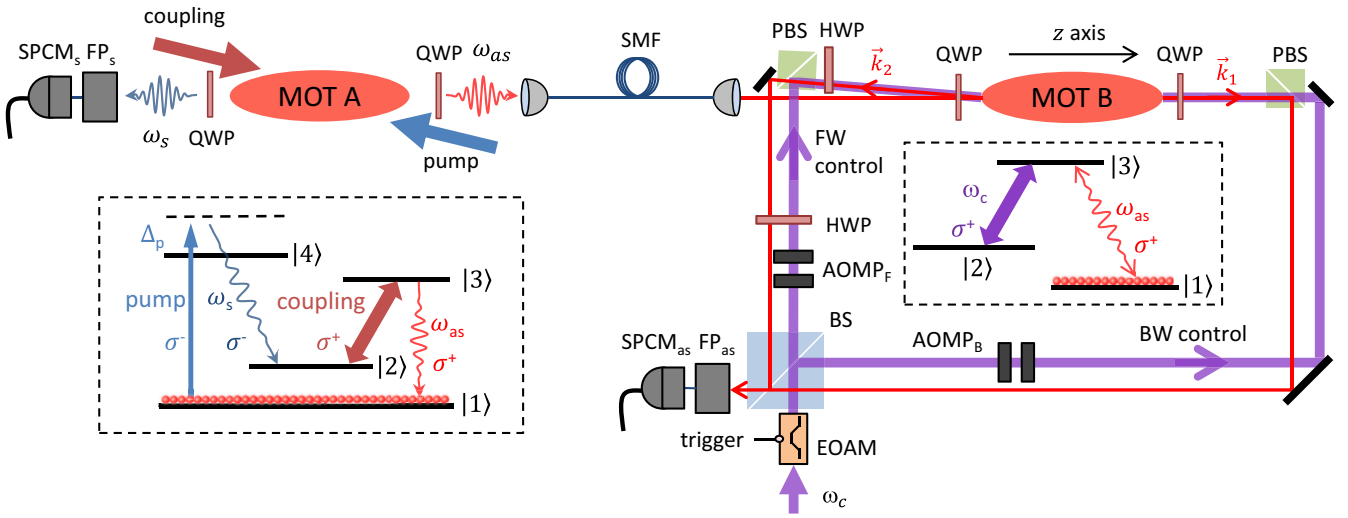


FIG. 1. Schematic of a single photon at a quantum-memory-based beam splitter (BS). Triggered by the detection of a Stokes photon ($\omega_s$) at the single-photon counting module SPCM$_s$, a heralded single anti-Stokes photon ($\omega_{as}$) is produced from SFWM in $^{85}$Rb magneto-optical trap (MOT) A. The anti-Stokes photon is then coupled into a single-mode fiber (SMF) and sent to cold $^{85}$Rb atoms in MOT B. With forward (FW) and backward (BW) control beams, the single-photon wave packet is stored and then retrieved into two spatial modes $\vec{k}_1$ and $\vec{k}_2$. The two output modes are combined at a conventional BS to form a Mach-Zehnder interferometer, whose output is measured by a second single-photon detector SPCM$_{as}$. FP$_s$ and FP$_{as}$ are Fabry-Perot filters with a bandwidth of 60 MHz. AOMP$_F$ and AOMP$_B$ are acousto-optic modulator pairs for controlling the amplitude and phase of the FW and BW control beams. The electro-optical amplitude modulator (EOAM) is used to switch on and off the control beams. The relevant $^{85}$Rb atomic energy levels are $|1\rangle = |5S_{1/2}, F = 2\rangle$, $|2\rangle = |5S_{1/2}, F = 3\rangle$, $|3\rangle = |5P_{1/2}, F = 3\rangle$, and $|4\rangle = |5P_{3/2}, F = 3\rangle$.

forward (FW) and backward (BW) control laser beams. The FW control beam is shined to MOT B with a small angle of 0.5° to the heralded anti-Stokes photon propagation direction ($+z$ axis), and the BW control beam counterpropagates toward the anti-Stokes photon. The storage-based BS mechanism can be described as follows. With the FW control laser beam on, it creates EIT, slows down, and compresses the anti-Stokes photon wave packet in MOT B. As the photon enters MOT B, we switch off the FW control beam and convert (or store) the photon into a long-lived atomic spin wave—this is the storage process. After a controllable time delay, we switch on both FW and BW control beams simultaneously—this process converts the stored atomic spin wave into a photonic state that is a superposition of two different momentum modes $|\vec{k}_1\rangle$ and $|\vec{k}_2\rangle$, as described in Eq. (1). The splitting process satisfies the phase-matching condition: $\vec{k}_1 = \vec{k}_{\rm in} - \vec{k}_{\rm FW} + \vec{k}_{\rm FW} = \vec{k}_{\rm in}$ and $\vec{k}_2 = \vec{k}_{\rm in} - \vec{k}_{\rm FW} + \vec{k}_{\rm BW} \simeq -\vec{k}_{\rm FW}$, where $\vec{k}$ represents the wave vector. The angle of 0.5° between $\vec{k}_{\rm FW}$ and $-\vec{k}_{\rm BW}$ is large enough to prevent the stationary light pulse effect [12,18].

## III. RESULTS

EIT optical storage and retrieval in forward and backward operations has been intensively studied in both experiment [19–21] and theory [22,23]. The temporal wave form of the heralded anti-Stokes photons generated from MOT A is shown as the black curve in Fig. 2(a), which has a coherence time of about 180 ns. The green dashed curve is the delayed wave form when the EIT slow light is present continuously (with a steady-state Rabi frequency of $2\pi \times 21$ MHz), which shows at $\tau = 200$ ns that the photon wave packet is mostly compressed

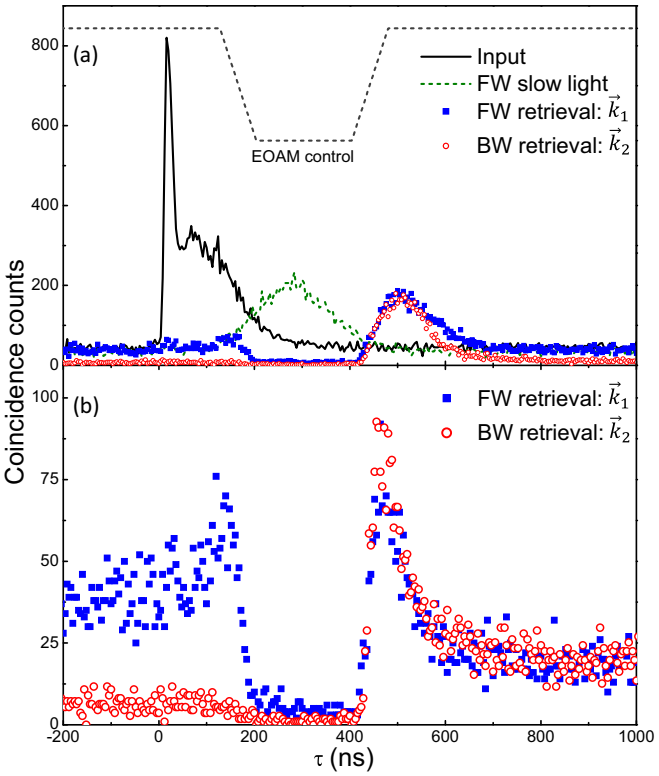


FIG. 2. Photon wave forms after the atomic BS measured as coincidence counts in 35 min with 4-ns time bin width. (a) FW or BW storage retrieval when only one retrieval (FW or BW) control beam is present. (b) BS output wave forms when both FW and BW retrieval control beams are present simultaneously.

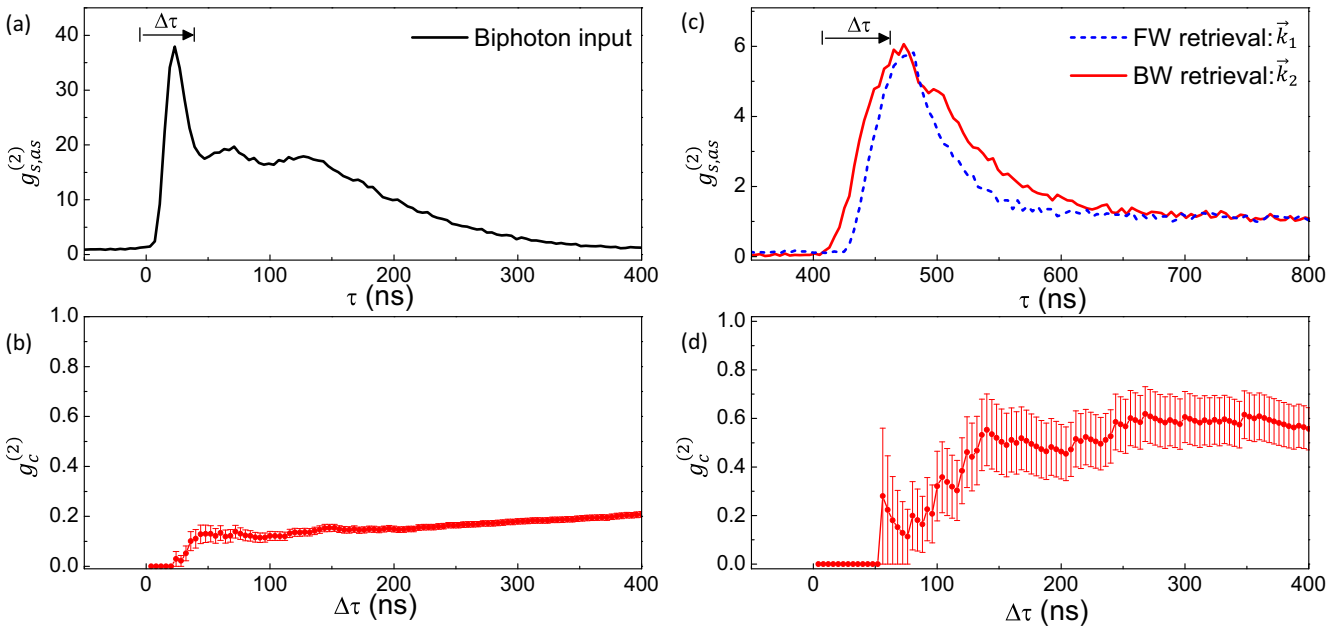


FIG. 3. Autocorrelation of a single-photon wave packet measured by a BS. (a) Incident anti-Stokes photon wave form and (b) its autocorrelation $g_c^{(2)}$ measured with a conventional BS as a function of the coincidence time window length $\Delta\tau$. (c) Retrieved anti-Stokes photon wave form and (d) its autocorrelation $g_c^{(2)}$ measured with the atomic BS.

inside the atomic medium. Then we adiabatically and linearly ramp down the power of the FW control beam from $\tau = 125$ to 200 ns, and store the photon state information into the atomic spin state. As the first step of realizing the BS, we need to balance the two retrieval outputs, which is crucial for a BS-based interferometer. To do so, we optimize the powers of FW and BW laser beams. The blue squares (or red circles) in Fig. 2(a) shows the retrieved photon wave form in the $\vec{k}_1$ (or $\vec{k}_2$) mode, when only one control beam (FW or BW) is switched on at $\tau = 400$ ns with a ramp time of 75 ns and the same Rabi frequency $\Omega_{\rm FW} = \Omega_{\rm BW} = 2\pi \times 21$ MHz. Figure 2(b) displays the $\vec{k}_1$ and $\vec{k}_2$ photon wave forms when both FW and BW control beams are switched on simultaneously. These two wave forms are nearly identical. Besides the loss caused by the finite dephasing between the two hyperfine ground levels $|1\rangle$ and $|2\rangle$, the spatial interference of the FW and BW beams introduces additional loss [24]. The total storage-retrieval efficiency in the BS operation is 28% [$\vec{k}_1$: $A^2\cos^2\theta = (13 \pm 2)\%$, $\vec{k}_2$: $A^2\sin^2\theta = (15 \pm 3)\%$]. From these data, we obtain the total transmission efficiency $A^2 = 0.28$ as defined in Eq. (1) with $\theta = \pi/4$. It is clear that in the FW $\vec{k}_1$ mode there is a leakage ($\tau < 200$ ns) resulting from the unstored part of the wave packet, which is not present in the BW $\vec{k}_2$ direction.

We first confirm that the atomic BS preserves the quantum particle nature of the heralded single photons by measuring their correlation function $g_c^{(2)} = \langle \hat{a}_1^\dagger \hat{a}_2^\dagger \hat{a}_2 \hat{a}_1 \rangle / (\langle \hat{a}_1^\dagger \hat{a}_1 \rangle \langle \hat{a}_2^\dagger \hat{a}_2 \rangle)$ between the two balanced output ports ($\theta = \pi/4$): A single-photon incident to a BS can only go to one output port or another. This question has not been addressed in the previous studies where atoms are used to split a coherent laser beam [11–13]. For a pure single-photon state, $g_c^{(2)} = 0$ because a single photon cannot be split into two. A two-photon Fock state gives $g_c^{(2)} = 0.5$ and a classical state gives $g_c^{(2)} \geqslant 1.0$. Figure 3(a) shows the temporal wave form of the heralded anti-Stokes

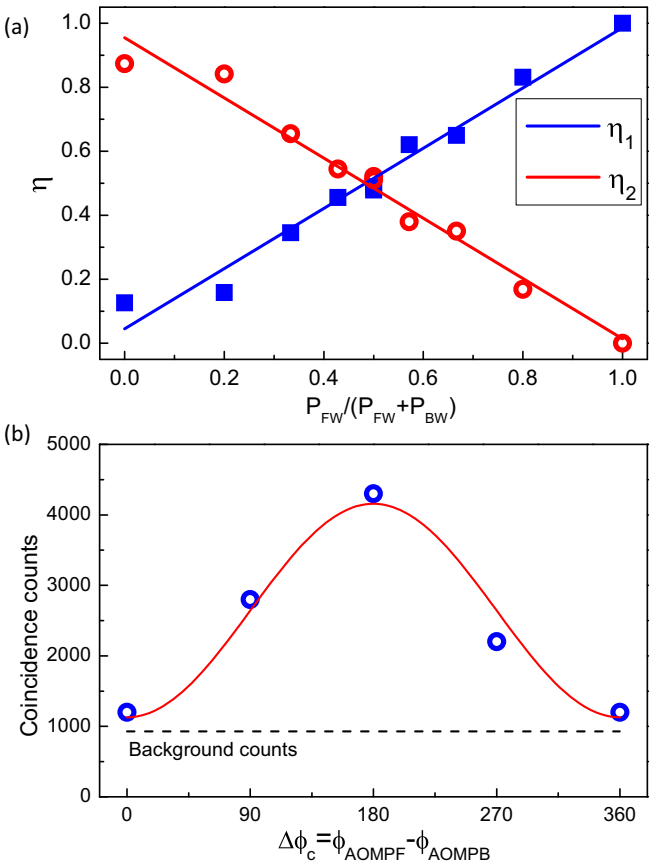


FIG. 4. (a) BS's FW and BW splitting ratios as functions of the FW control laser power. (b) Single-photon MZ interference result by varying the AOM-pair phase difference. The coincidence counts are measured over a 200-ns coincidence time window and total time of 300 min.

photons. The measured conditional (or heralded) correlation function of these input photons after a conventional BS as a function of coincidence bin width $\Delta\tau$ is shown in Fig. 3(b), which shows $g_c^{(2)} < 0.5$ (below the two-photon threshold) within the entire photon coherence time and confirms the single-photon nature of the input photons. Figure 3(c) shows the temporal wave forms of the heralded anti-Stokes photons in the $\vec{k}_1$ and $\vec{k}_2$ modes after the BS. $g_c^{(2)} < 0.5$ is well preserved for $\Delta\tau \leqslant 150$ ns. For 150 ns $\leqslant \Delta\tau \leqslant 400$ ns, $g_c^{(2)}$ degrades because of the noise photon counts but it is still below the classical limit of 1.0. Therefore, we have confirmed the particle nature of a single photon preserved at the BS.

The splitting ratio $\eta_1 = \cos^2\theta$ and $\eta_2 = \sin^2\theta$ can be controlled by varying the powers of the FW and BW retrieved beams. The measured results of $\eta_1$ and $\eta_2$ as functions of $P_{\rm FW}/(P_{\rm FW} + P_{\rm BW})$ are plotted in Fig. 4(a), where the solid lines are linear fits and agree well with the following relations: $\eta_1 = \cos^2\theta = P_{\rm FW}/(P_{\rm FW} + P_{\rm BW})$ and $\eta_2 = \sin^2\theta = 1 - P_{\rm FW}/(P_{\rm FW} + P_{\rm BW})$.

Another important property of a BS is preservation of phase coherence in Eq. (1). In the EIT storage process, the atomic spin state is prepared by the FW control laser beam and the input photon so that reversible retrieval in the $\vec{k}_1$ and $\vec{k}_2$ directions become possible. These phase-matching processes indicate the BS operation is a coherent process. The relative phase $\varphi$ between the two output ports is determined by the phase difference between the FW and BW control beams when they meet at MOT B:

$$\varphi = (\phi_{\rm LF} + \phi_{\rm AOMPF}) - (\phi_{\rm LB} + \phi_{\rm AOMPB}), \tag{2}$$

where $\phi_{\rm LF}$ and $\phi_{\rm LB}$ are path-length phases of the FW and BW beams propagating from the 50:50 BS to MOT B (Fig. 1). $\phi_{\rm AOMPF}$ and $\phi_{\rm AOMPB}$ are the phases introduced by the two AOM pairs which can be precisely controlled by their driving radio-frequency sources. We construct a MZ interferometer to confirm the coherence of the atomic BS. As shown in Fig. 1, the two outputs of the atomic BS are directed and combined at the conventional BS that is used for splitting the control beam, and the interference output is detected by the photon counter $\rm SPCM_{\it as}$. Figure 4(b) shows the coincidence counts between $\rm SPCM_{\it s}$ and $\rm SPCM_{\it as}$ as a function of $\Delta\phi_c = \phi_{\rm AOMPF} - \phi_{\rm AOMPB}$ when the atomic BS is operated under the balance output mode ($\theta = \pi/4$). The solid line is the best fitted sinusoidal curve, and the dashed line is the background accidental coincidence from stray light and detector dark counts. Subtracting this background noise, we obtain a visibility of 89% for the interference signal, which is limited by the mismatch of retrieval wave forms and stability of the residual phases. This high interference visibility confirms the coherence of the atomic BS. As we actually send a single-photon wave packet into the atomic BS, the interference result reveals the wave nature of the single photons. That is, the output single anti-Stokes photon state is a coherent superposition of the $\vec{k}_1$ and $\vec{k}_2$ modes.

## IV. SUMMARY

In summary, we demonstrate a configurable single-photon BS based on EIT storage in cold atoms. Using narrow-band heralded single photons, we show that such a BS preserves the particle-wave duality of photons. We observed the anti-bunching effect of single photons at the atomic BS in their autocorrelation. The phase coherence between the two split modes is confirmed with a single-photon MZ interferometer. The splitting ratio and phase can be dynamically controlled with the control beams and the atomic parameters. We note that the total transmission efficiency (28%) is low in this proof-of-principle demonstration. This problem is caused by the low storage-retrieval efficiency and can be improved by minimizing the atomic ground-state dephasing. For example, an EIT quantum memory with an efficiency of >90% has been recently achieved [25]. This quantum-memory-based controllable BS may have applications in a quantum information processing network. It can also be used for testing some fundamental quantum physics, such as Wheeler's delayed-choice experiment [26].

## ACKNOWLEDGMENT

This work was supported by Hong Kong Research Grants Council (Project No. 16304817).

[1] A. Zeilinger, General properties of lossless beam splitters in interferometry, Am. J. Phys. **49**, 882 (1981).
[2] B. Yurke, S. L. McCall, and J. R. Klauder, *SU* (2) and *SU* (1, 1) interferometers, Phys. Rev. A **33**, 4033 (1986).
[3] M. Born and E. Wolf, *Principles of Optics* (Elsevier, Amsterdam, 2013).
[4] E. J. Post, Sagnac effect, Rev. Mod. Phys. **39**, 475 (1967).
[5] R. H. Brown and R. Q. Twiss, Correlation between photons in two coherent beams of light, Nature (London) **177**, 27 (1956).
[6] C. K. Hong, Z. Y. Ou, and L. Mandel, Measurement of subpicosecond time intervals between two photons by interference, Phys. Rev. Lett. **59**, 2044 (1987).
[7] J.-W. Pan, Z.-B. Chen, C.-Y. Lu, H. Weinfurter, A. Zeilinger, and M. Zukowski, Multiphoton entanglement and interferometry, Rev. Mod. Phys. **84**, 777 (2012).
[8] P. Kok, W. J. Munro, K. Nemoto, T. C. Ralph, J. P. Dowling, and G. J. Milburn, Linear optical quantum computing with photonic qubits, Rev. Mod. Phys. **79**, 135 (2007).
[9] H. J. Kimble, The quantum internet, Nature (London) **453**, 1023 (2008).
[10] N. Sangouard, C. Simon, H. De Riedmatten, and N. Gisin, Quantum repeaters based on atomic ensembles and linear optics, Rev. Mod. Phys. **83**, 33 (2011).
[11] K. F. Reim, J. Nunn, X. M. Jin, P. S. Michelberger, T. F. M. Champion, D. G. England, K. C. Lee, W. S. Kolthammer, N. K. Langford, and I. A. Walmsley, Multipulse Addressing of a Raman Quantum Memory: Configurable Beam Splitting and Efficient Readout, Phys. Rev. Lett. **108**, 263602 (2012).
[12] K. K. Park, T. M. Zhao, J. C. Lee, Y. T. Chough, and Y. H. Kim, Coherent and dynamic beam splitting based on light storage in cold atoms, Sci. Rep. **6**, 34279 (2016).

[13] Y. Xiao, M. Klein, M. Hohensee, L. Jiang, D. F. Phillips, M. Lukin, and R. L. Walsworth, Slow Light Beamsplitter, Phys. Rev. Lett. **101**, 043601 (2008).

[14] L. Zhao, X. Guo, C. Liu, Y. Sun, M. M. T. Loy, and S. Du, Photon pairs with coherence time exceeding one microsecond, Optica **1**, 84 (2014).

[15] S. Du, J. Wen, and M. H. Rubin, Narrowband biphoton generation near atomic resonance, J. Opt. Soc. Am. B **25**, C98 (2008).

[16] S. Du, Quantum-state purity of heralded single photons produced from frequency-anticorrelated biphotons, Phys. Rev. A **92**, 043836 (2015).

[17] P. Qian, Z. Gu, R. Cao, R. Wen, Z. Y. Ou, J. F. Chen, and W. Zhang, Temporal Purity and Quantum Interference of Single Photons From Two Independent Cold Atomic Ensembles, Phys. Rev. Lett. **117**, 013602 (2016).

[18] Y.-W. Lin, W.-T. Liao, T. Peters, H.-C. Chou, J.-S. Wang, H.-W. Cho, P.-C. Kuan, and I. A. Yu, Stationary Light Pulses in Cold Atomic Media and Without Bragg Gratings, Phys. Rev. Lett. **102**, 213601 (2009).

[19] S. Zhang, S. Zhou, M. M. T. Loy, G. K. L. Wong, and S. Du, Optical storage with electromagnetically induced transparency in a dense cold atomic ensemble, Opt. Lett. **36**, 4530 (2011).

[20] Y.-H. Chen, M.-J. Lee, I-C. Wang, S. Du, Y.-F. Chen, Y.-C. Chen, and I. A. Yu, Coherent Optical Memory with High Storage Efficiency and Large Fractional Delay, Phys. Rev. Lett. **110**, 083601 (2013).

[21] S. Zhou, S. Zhang, C. Liu, J. F. Chen, M. M. T. Loy, G. K. L. Wong, and S. Du, Optimal storage and retrieval of single-photon waveforms, Opt. Express **20**, 24124 (2012).

[22] A. V. Gorshkov, A. Andre, M. Fleischhauer, A. S. Sørensen, and M. D. Lukin, Universal Approach to Optimal Photon Storage in Atomic Media, Phys. Rev. Lett. **98**, 123601 (2007).

[23] M. Fleischhauer, A. Imamoglu, and J. P. Marangos, Electromagnetically induced transparency: Optics in coherent media, Rev. Mod. Phys. **77**, 633 (2005).

[24] H. Y. Ling, Y. Q. Li, and M. Xiao, Electromagnetically induced grating: Homogeneously broadened medium, Phys. Rev. A **57**, 1338 (1998).

[25] Y.-F. Hsiao, P.-J. Tsai, H.-S. Chen, S.-X. Lin, C.-C. Hung, C.-H. Lee, Y.-H. Chen, Y.-F. Chen, I. A. Yu, and Y.-C. Chen, Highly Efficient Coherent Optical Memory Based on Electromagnetically Induced Transparency, Phys. Rev. Lett. **120**, 183602 (2018).

[26] X.-S. Ma, J. Kofler, and A. Zeilinger, Delayed-choice gedanken experiments and their realizations, Rev. Mod. Phys. **88**, 015005 (2016).